

Experimental Determination of Fouling Characteristics of Malaysian Crude Oil

by

Nur Adilah bt Muhammad Adib

8703

Dissertation submitted in partial fulfilment of
the requirements for the
Bachelor of Engineering (Hons)
(Chemical Engineering)

JANUARY 2010

Supervisor: AP DR Marappagounder Ramasamy

Universiti Teknologi PETRONAS
Bandar Seri Iskandar
31750 Tronoh
Perak Darul Ridzuan

CERTIFICATION OF APPROVAL

Experimental Determination of Fouling Characteristics of Malaysian Crude Oil

by

Nur Adilah bt Muhammad Adib

A project dissertation submitted to the
Chemical Engineering Programme
Universiti Teknologi PETRONAS
in partial fulfilment of the requirement for the
BACHELOR OF ENGINEERING (Hons)
(CHEMICAL ENGINEERING)

Approved by,


10/06/2010
(AP DR Marappagounder Ramasamy)

UNIVERSITI TEKNOLOGI PETRONAS

TRONOH, PERAK

January 2010

CERTIFICATION OF ORIGINALITY

This is to certify that I am responsible for the work submitted in this project, that the original work is my own except as specified in the references and acknowledgements, and that the original work contained herein have not been undertaken or done by unspecified sources or persons.



NUR ADILAH BT MUHAMMAD ADIB

ABSTRACT

Malaysian crude oils used to pose very little fouling problems, however as time progresses, the fouling problem became more and more prominent in the crude oil. This project concentrates on chemical fouling resulting from running the Malaysian crude oil in the Hot Liquid Process Simulator 320 (HLPS-320). Six experiments were conducted by heating crude oil in the HLPS under N₂ pressure of 3.4 MPa. The HLPS will run on varying bulk temperatures from 70°C to 100°C and surface temperatures from 220°C to 260°C at constant pressure and velocity. Results from the experiment will be used in Excel spreadsheet to calculate fouling resistance which was based on semi-log plot of Arrhenius equation. Initial fouling rates are then compared for different bulk temperatures and surface temperatures. The experiment results will then be fitted to the calculated date from the Ebert-Panchal's model of threshold fouling. Results show that there is a strong correlation between bulk temperatures, surface temperatures and the subsequent fouling rates.

TABLE OF CONTENTS

ACKNOWLEDGEMENTS.....	I
LIST OF FIGURES.....	II
LIST OF TABLES.....	III
CHAPTER 1: INTRODUCTION	1
1.1 Problem statement.....	1
1.2 Objectives.....	2
1.3 Scope of work.....	2
1.4 Background studies.....	3
1.4.1 Particulate fouling.....	3
1.4.2 Precipitation fouling.....	3
1.4.3 Chemical reaction fouling.....	4
1.4.4 Biological fouling.....	4
1.4.5 Corrosion fouling.....	4
1.4.6 Solidification fouling.....	4
1.4.7 Chemical reactions leading to fouling.....	5
CHAPTER 2: LITERATURE REVIEW	6
2.1 Semi-empirical fouling models.....	9
CHAPTER 3: METHODOLOGY	12
3.1 Material.....	12

3.2	Crude oil properties	13
3.3	Apparatus.....	13
3.4	Operating procedures	17
3.5	Experimental procedures.....	18
3.5.1	Sample preparation.....	18
3.5.2	Pre-heat up and pressurization	18
3.5.3	HLPS power-up.....	19
3.5.4	Fouling runs and data recording.....	19
3.5.5	Shut down.....	19
3.5.6	Washing run of HLPS	19
3.5	PROGRESS AND MILESTONES.....	20
CHAPTER 4: RESULTS AND DISCUSSION.....		22
4.1	Results	22
4.2	Effect of bulk temperature.....	26
4.3	Effect of surface temperature.....	30
CHAPTER 5: CONCLUSION AND RECOMMENDATIONS.....		38
5.1	Conclusions.....	38
5.2	Recommendations.....	39
REFERENCES		40
APPENDIX		41

ACKNOWLEDGEMENTS

Foremost I would like to thank my supervisor, A.P. Dr Marappagounder Ramasamy, for his patience, support and guidance throughout the duration of this Final Year Project. I would like to thank the lab technician and postgraduate student for their technical support. I am also thankful to the chemical engineering department, and my friends for their support.

LIST OF FIGURES

Figure 1: Fouling resistance in shell and tube heat exchangers.....	7
Figure 2: Total annual cost of a double pipe heat exchanger arrangement.....	8
Figure 3: Comparison of experimental and fitted fouling rates of crude oil by Ebert and Panchal (1997).....	10
Figure 4: Wall temperature vs. velocity.....	10
Figure 5: Schematic diagram of Hot Liquid Process Simulator 320 loop.	14
Figure 6: Experimental set-up of Hot Liquid Process Simulator 320.....	14
Figure 7: Heater tube with clean surface before the experiment.	14
Figure 8: HLPS Heater System Controller.....	15
Figure 9: Feed tank.....	15
Figure 10: Basic Alcor's HLPS 320 System.....	16
Figure 11: Picture of a fouled probe after the experiment.....	22
Figure 12: Comparison of fouling rates at bulk temperatures 70°C, 80°C and 100°C with $T_s=260^\circ\text{C}$	27
Figure 13: Experimental results at constant $T_s=260^\circ\text{C}$ fitted to Ebert-Panchal model of fouling threshold.....	28
Figure 14: Fouling resistance plotted against time at $T_b=70^\circ\text{C}$ for surface temperatures of 220°C, 240°C, and 260°C.....	30
Figure 15: Fouling resistance plotted against time at $T_b=80^\circ\text{C}$ for surface temperatures of 220°C, 240°C, and 260°C.....	31
Figure 16: Fouling resistance plotted against time at $T_b=100^\circ\text{C}$ for surface temperatures of 220°C, 240°C, and 260°C.....	32
Figure 18: Arrhenius plot of fouling rate versus inverse film temperature at constant $T_b=80^\circ\text{C}$	33
Figure 19: Experimental results at constant $T_b=80^\circ\text{C}$ fitted to Ebert-Panchal model of fouling threshold.	34

LIST OF TABLES

Table 1: Type of fouling of heat exchangers in various industries	5
Table 2: Properties of the Malaysian crude oil.....	13
Table 3: Progress and Milestone of the Project.....	20
Table 4: Progress and Milestone of the Project (continued)	21
Table 5: Initial fouling rates at constant $T_s=260^\circ\text{C}$ and bulk temperatures 70°C , 80°C and 100°C	26
Table 6: Experimental and predicted initial fouling rates for constant $T_s=260^\circ\text{C}$	28
Table 7: Summary of results at varying bulk temperatures at $T_s=260^\circ\text{C}$	29
Table 8: Initial fouling rates at constant bulk temperature of 70°C	30
Table 9: Initial fouling rates at constant bulk temperature of 80°C	31
Table 10: Initial fouling rates at constant bulk temperature of 100°C	31
Table 11: Log values of initial fouling rates at constant $T_b=80^\circ\text{C}$	33
Table 12: Experimental and predicted initial fouling rates at constant bulk temperature $T_b=80^\circ\text{C}$	34
Table 13: Summary of results at varying surface temperatures at $T_b=70^\circ\text{C}$	35
Table 14: Summary of results at varying surface temperatures at $T_b=80^\circ\text{C}$	36
Table 15: Summary of results at varying surface temperatures at $T_b=100^\circ\text{C}$	37

CHAPTER 1

INTRODUCTION

1.1 PROBLEM STATEMENT

The aim of this project is to study fouling characteristics of a Malaysian crude oil in the Alcor Hot Liquid Process Simulator 320 (HLPS 320). Malaysian crude oil is known for its low asphaltene content, nevertheless susceptible to the fouling deposition which has somewhat become a big problem over the last few years.

In a petroleum refinery, profit losses occur due to fouling of crude oil and blends in the heat exchanger. It is important to know that the characteristics of fouling are influenced by several operating parameters such as temperature, pressure and flow velocity. To mitigate fouling, the mechanisms have to be understood and countermeasures need to be identified.

As of late, countless research has been done to determine fouling characteristics in crude oils. Nonetheless, steps taken to mitigate fouling have not been able to completely eliminate deposition on the surface of heat exchangers, but rather minimize fouling up to shut down for cleaning.

This project will concentrate more on chemical reaction fouling aspects which is the dominant fouling mechanism during heat exchange process. All experiments in this project are conducted on the Alcor Hot Liquid Process Simulator 320 (HLPS320) using Malaysian crude oil blends with varied wall temperatures, at constant velocity. Results of experimental data obtained from experimental work might give an insight towards minimizing the effects of real life application fouling.

1.2 OBJECTIVES

- To determine fouling characteristics of a Malaysian crude oil using HLPS equipment
- To study effect of surface temperature and bulk temperature on fouling rates
- To determine best operating film and surface temperature to mitigate fouling
- To fit experimental data to Ebert and Panchal fouling model

1.3 SCOPE OF WORK

The project will take place in the form of laboratory experiments. The experiments will be held at the fouling research lab, in block P. Hot Liquid Process Simulator (HLPS) will be the equipment used to study fouling characteristics of a Malaysian crude oil. The results will be used to calculate fouling resistance. Then the results of the experiment will be fitted into the Ebert-Panchal model of threshold fouling using excel solver.

1.4 BACKGROUND STUDIES

Mass balance for fouling is as follows:

$$\text{Accumulation} = \text{Input} - \text{Output}$$

Or in more precise mathematical terms:

$$\frac{dm}{dt} = \phi_D - \phi_R$$

m is the mass of deposit per meter²

ϕ_D and ϕ_R are the deposit and removal mass flow rates per unit area of surface respectively.

There are six types of fouling by which deposits may be created. They are (1) particulate fouling, (2) precipitation fouling, (3) chemical reaction fouling, (4) biological fouling, (5) Corrosion fouling and (6) Solidification fouling. In real industrial settings, two or more fouling mechanisms could occur in conjunction in a given process. Types of fouling that bred problems in equipments are explained below and shown in figure 1.

1.4.1 Particulate fouling

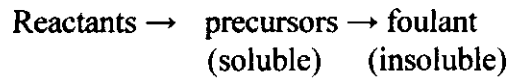
Particulate fouling occurs when small suspended particles deposits such as clay, silt or iron oxide deposits on a heat transfer surface of any orientation.

1.4.2 Precipitation fouling

Precipitation fouling occurs when dissolved salts deposit on a heat transfer surface due to supersaturation caused by: evaporation of solvent, cooling below solubility limit, and mixing of streams with different compositions.

1.4.3 Chemical reaction fouling

Chemical reaction fouling is the deposit formation by a chemical reaction by which the surface of heat exchangers do not interfere in the fouling process. Chemical reaction fouling generally involves the following process:



1.4.4 Biological fouling

Biological fouling is the accumulation of living matter whether deposition or growth on equipment surfaces due to optimum temperature for biological activity. This type of fouling can be divided into two—fouling by micro organisms or by macro organisms. Examples of micro organisms are bacteria, algae and fungi, while examples of macro organisms are mussels, barnacles, hydroids and seaweed.

1.4.5 Corrosion fouling

Corrosion fouling occurs when the surface of the equipments deteriorates due to some form of chemical attack. The presence of corrosion products represents a resistance to heat transfer and therefore amount to a fouling deposit.

1.4.6 Solidification fouling

Solidification fouling happens when the liquid freezes when flowing through equipment below freezing point of the liquid. The presence of a solid layer hinders heat removal from the flowing liquid.

Fouling deposition in the processing of a crude oil involves chemical reaction, particulate and corrosion fouling; with chemical reaction fouling as the predominant type of fouling.

1.4.7 Chemical reactions leading to fouling

The following are mechanisms that could explain deposition by chemical reactions. (Watkinson et al, 1997):

- a) *Gum formation.* A soluble oxidation product forms by autoxidation with further oxidation to an insoluble polymer. The polymer may be formed on the wall or transported as particles to the wall.
- b) *Deposition of asphaltenes.* Precipitation and adherence to heat transfer surfaces is caused by the incompatibility of asphaltenes with crude oil through reactions or insolubility.
- c) *Thermal decomposition.* Ionic decomposition requires more energy than decomposition via radical formation so that thermal cracking proceeds through the free radical route.
- d) *Coke formation.* Coke forms in ethylene and propylene by cyclisation with higher olefins and aromatics. This mechanism also occurs in heating heavy organics in the absence of oxygen.

Industry Group	Type of Fouling	Extent of Problem
Food and kindred products	Chemical reaction Crystallisation Biological Particulate Corrosion	Major Major Medium Minor/Major Minor
Textile mill products	Particulate Biological	
Wood and paper products	Crystallisation Particulate Biological Chemical reaction Corrosion	Major Minor Minor Minor Medium Medium
Chemical and allied industries	Crystallisation Particulate Biological Chemical reaction Corrosion	Minor/Medium Medium Minor/Major Medium
Petroleum refineries	Chemical reaction Crystallisation Particulate Biological Corrosion	Major Medium Minor/Medium Medium Medium
Tone, glass, concrete	Particulate	Minor/Major
Electricity generation	Biological Crystallisation Particulate Freezing Corrosion	Major Medium Major Major Minor

Table 1: Type of fouling of heat exchangers in various industries

CHAPTER 2

LITERATURE REVIEW

Fouling is defined as the deposition of unwanted particles at the surface of heat exchangers. (Bott, 1994) Fouling in crude oil preheat train causes monetary losses in terms of maintenance, energy and lost production. Fouling, which causes reduced efficiency in heat exchangers will not only increase the usage of fuel, but also impacts the conservation of the world's energy resources. The use of extra fossil fuel will affect the environment and carbon dioxide produced will add to the global warming effect.

Fouling also causes pressure drop problems. The pressure drop will increase with the presence of foulant that restrict the flow in the heat exchanger. Worst case scenario is that the heat exchanger is rendered inoperable because of the back pressure. Reduced efficiency in heat exchangers caused by fouling will result in more consumption of fuel. Fouling also causes equipment shut-downs and subsequently the loss of production and profit.

The financial losses incurred due to fouling of crude oil in the pre-heat exchanger a crude oil process refinery reaches up to millions of dollars per year. (Bott, 1995) A mail survey from New Zealand companies showed that 90% of heat exchangers suffer from fouling problems. (Müller-Steinhagen, 2000) Heat exchangers are built to be larger to compensate for the blockage of fouling deposition. This step, however does not remedy the deposition of particles. The extra surface area will cause an increase in capital cost. According to Hans Müller-Steinhagen (2000), 40% out of 80% of oversized heat exchangers can be attributed to fouling.

Operating conditions is found to play a role in the fouling process. The following process parameters influence fouling (Wilson *et al*, 2005):

- i) Fouling rates increases with the increasing surface temperature.
- ii) Fouling decreases with the increasing flow velocity.

In a study conducted by M. Srinivasan (2004), at bulk temperatures over the range 200-285°C and initial surface temperatures from 300 to 380°C, a few findings that are in agreement with Wilson *et al*'s work are shown below:

- i. A 28°C increase in film temperature causes the fouling rate to double.
- ii. The fouling rate decreased as the velocity was increased to the power -0.35.
- iii. The fouling rate could be correlated using a modified film temperature which gave more weight to the surface temperature than to the bulk temperature.
- iv. The deposits were rich in mineral matter and in sulphur.
- v. The fouling rates at fixed velocity were highest with the heaviest oil.

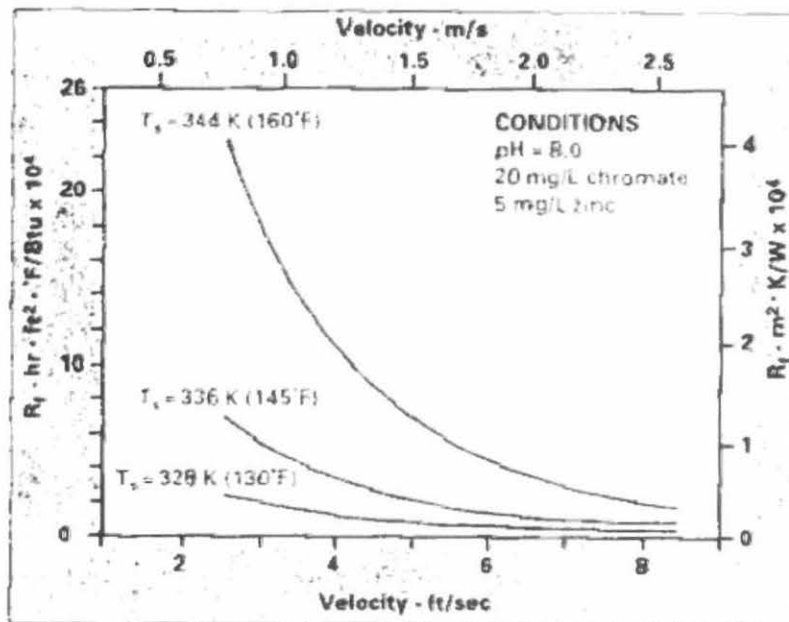


Figure 1: Fouling resistance in shell and tube heat exchangers

(Source: Muller-Steinhagen, 2000)

Figure 1 illustrates fouling resistance as a function of flow velocity and surface temperature in shell and tube heat exchangers. Fouling resistance is relatively

low at 55°C compared to fouling resistance at 71°C with both having velocity of 0.6 m/s. This happens to be the case as the velocity shifted higher, however there is a significant amount of decrease in fouling resistance at every temperature as velocity increases.

Even with advances in fouling research over the past 2 decades, there is no fixed solution to fouling in heat exchangers. The same rule does not apply to every heat exchanger, even though they could significantly improve some heat exchanger optimization procedures. This is explained in figure 2, which shows the total cost of operating a double pipe heat exchanger as a function of flow velocity. The first curve has a constant fouling resistance while the second curve is velocity dependent. With fouling resistance dependent on velocity, the optimal flow velocity increases to approximately 1.2 m/s compared to 0.7 m/s and reduces total cost by 10%.

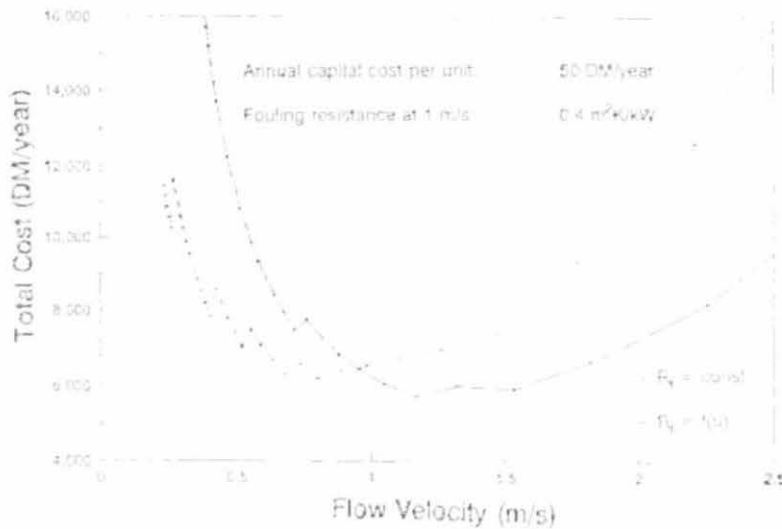


Figure 2: Total annual cost of a double pipe heat exchanger arrangement
(Source: Müller-Steinhagen, 2000)

Crude oil fouling is generally believed to be caused by impurities in the crude oil such as corrosion products, water and salt, by asphaltenes exceeding their solubility limit, or by thermal decomposition or autoxidation of reactive constituents in the oil. Asphaltene precipitation is considered to be a major cause of crude unit fouling. As well, reactive constituents of oil may undergo thermal decomposition, polymerization, or autoxidation reactions to produce fouling precursors or foulants

(Murphy and Campbell, 1992). Dickakian (1997) has shown the role of asphaltene and polar molecules in fouling at elevated temperatures where coke is produced following phase separation. At lower temperatures, asphaltene precipitation occurs due to changes in solvent nature via blending, or pressure change.

2.1 SEMI-EMPIRICAL FOULING MODELS

In 1995, Ebert and Panchal introduced a semi-empirical approach to quantify the effect of flow velocity on tube-side fouling in crude oils at high temperatures. They suggest that a combination of low temperature and high shear stress will produce a threshold condition such that the fouling rate will be essentially zero, which is also known as 'fouling threshold' (Wilson *et al*, 2005). Scarborough *et al*'s data was fitted to a numerical form to give

$$\begin{aligned} \frac{dR_f}{dt} &= \text{deposition} - \text{suppression} \\ &= A Re^{-\beta} \exp\left(\frac{-E}{RT_f}\right) - C\tau \quad [1] \end{aligned}$$

Whereby

- $A = 30.2 \times 10^6 \text{ K m}^2/\text{kW h}$
- $\beta = -0.88$
- $E = 68 \text{ KJ/mol}$
- $C = 1.45 \times 10^{-4} \text{ m}^2 \text{ K m}^2/\text{kW Pa h}$

The deposition depends on the temperature of the wall surface. The removal rate depends on flow velocity. A higher rate of deposition compared to rate of removal will result in significant fouling.

Conversely, when removal is more than deposition, fouling will be negligible. When deposition equals to formation, the fouling rate equals to zero (fouling threshold). Figure 3 shows the Ebert-Panchal model [1] fitted to Scarborough's data.

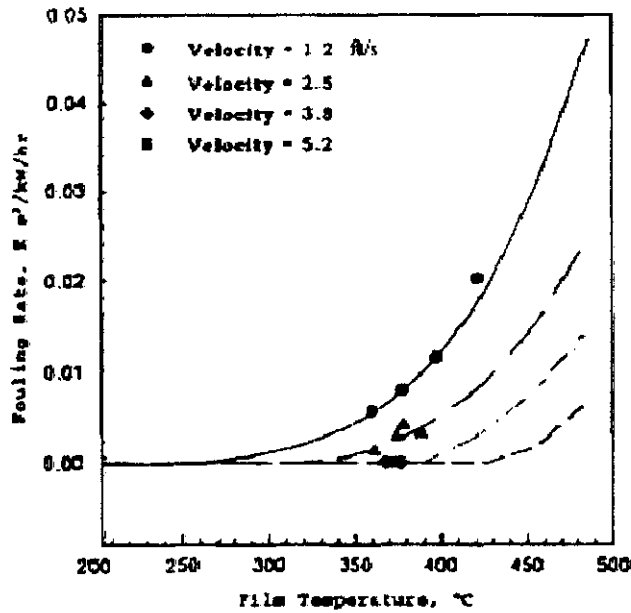


Figure 3: Comparison of experimental and fitted fouling rates of crude oil by Ebert and Panchal (1997)

The fouling threshold should be taken as the maximum wall temperature for a certain velocity. Below the threshold, no significant fouling occurs. Above the threshold, significant fouling can be expected, with severity of fouling increasing as the conditions move away from the threshold. This is shown in figure 4.

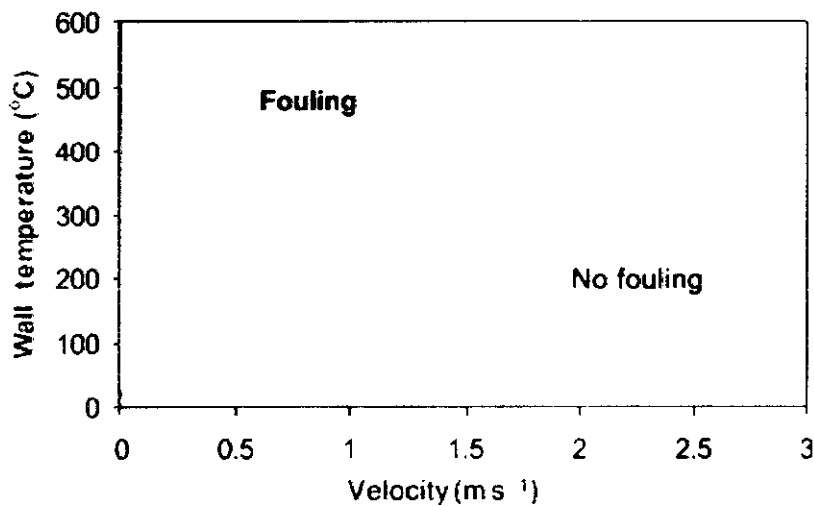


Figure 4: Wall temperature vs. velocity

Panchal revised the model (Wilson et al, 2005) (D.I. Wilson, 2005), which gives

$$\frac{dRf}{dt} = A_{II} Re^{-0.66} Pr^{-0.33} \exp\left[\frac{-E_{II}}{RT_f}\right] - C_{II}\tau_w \quad [2]$$

where A, E and C are adjustable parameters. Prandtl number and Reynolds number are introduced into the empirical model. The two non dimensional parameters account for fluid flow and thermal properties.

Polley *et al* (2002) argued that the depositional term is dependent on wall surface temperature, T_s rather than film temperature, T_f . He proposed another threshold model of fouling where the removal term is linked to the rate of convective mass transfer from the bulk liquid to the surface.

$$\frac{dRf}{dt} = A_{III} Re^{-0.8} Pr^{-0.33} \exp\left[\frac{-E_{III}}{RT_s}\right] - C_{III}Re^{0.8} \quad [3]$$

This model is said to have better agreement with Panchal *et al*'s data sets. (Yeap *et al*, 2004)

Epstein model for tube side chemical reaction fouling is as following

$$\frac{dRf}{dt} = \frac{A_{IV}C_f u T_s^{2/3} \rho^{2/3} \mu^{-4/3}}{1 + B_{IV}u^3 C_f^2 \rho^{5/3} \mu^{-7/3} T_s^{2/3} \exp\left(\frac{E_{IV}}{RT_s}\right)} - C_{IV}u^{0.8} \quad [4]$$

This model shows two temperature dependencies and three velocity dependencies in the term $C_f u$, $C_f^2 u^3$ and $C_{IV}u^{0.8}$. The model can vary the dependency of velocity by adjusting B_{IV} values. This model is said to be in best agreement with a depositional term compared to different terms for a larger data set. (YEAP *et al*, 2004)

CHAPTER 3

METHODOLOGY

3.1 MATERIAL

Malaysian crude oil will be used in the Hot Liquid Process Simulator. The purpose of testing crude oil using HLPS is basically to find out the fouling condition of the heat exchanger device. The heater tube is used to resemble the heat transfer device of the refinery plant. In this test, the sample, which is the crude oil, is heated and the heat from the sample is transferred through the tube's surface. The thermocouple will detect the temperature of this tube's surface to give the value from the temperature indicator.

This test will run for six hours with data taken in 15 minutes intervals. The main concern is to ensure the inlet temperature, T_1 and surface temperature at the tube length of 38 mm, T_c are at desired temperature whereby $T_1 = 80^\circ\text{C}$ and $T_c = 260^\circ\text{C}$. The nitrogen gas is the chosen inert gas which serves to speed up the process and to prevent the crude oil from vaporizing out of the HLPS. Nitrogen is inserted at the pressure of about 3.4 MPa. These data are to be taken every 15 minutes:

- A - Jacket heater of reservoir
- B - Pump
- C - Line heater
- T_1 - Inlet temperature
- T_2 - Outlet temperature
- $T_c@ 38 \text{ mm}$ - Surface temperature
- $T_c@10,20,30,40,50,60 \text{ mm}$ - Surface temperature

These data will be transferred into spreadsheet for further evaluation. The evaluated data from spreadsheet will then be fitted to the Ebert and Panchal threshold fouling model to estimate whether the result is pertinent to the model.

3.2 CRUDE OIL PROPERTIES

Only one type of crude oil will be used in the experiment. These are the properties of each individual crude oil:

No.	Test	D
1	Density @ 15°C (kg/L)	0.8435
2	API Gravity	36.2
3	Conradson Carbon (wt%)	0.88
4	Viscosity cSt @ 15°C	3.7
5	Total Sulphur (wt%)	0.062
6	Pour Point (°F)	-6
7	Asphaltene (wt%)	0.2

Table 2: Properties of the Malaysian crude oil

3.3 APPARATUS

This project utilizes usage of Alcor Hot Liquid Process Simulator 320 (HLPS 320) to carry out experimentation on chosen Malaysian crude oil. The Alcor HLPS 320 equipment allows experimentation of fouling to be conducted under a broad range of monitored conditions including temperature, pressure and flow rate. The crude oil will pass through a resistance heated tube-in-shell heat exchanger while the conditions above are monitored. The heater tube is 2 mm in diameter. The schematic diagram of HLPS 320 is shown below (figure 3) and the basic HLPS 320 system is shown in figure 4.

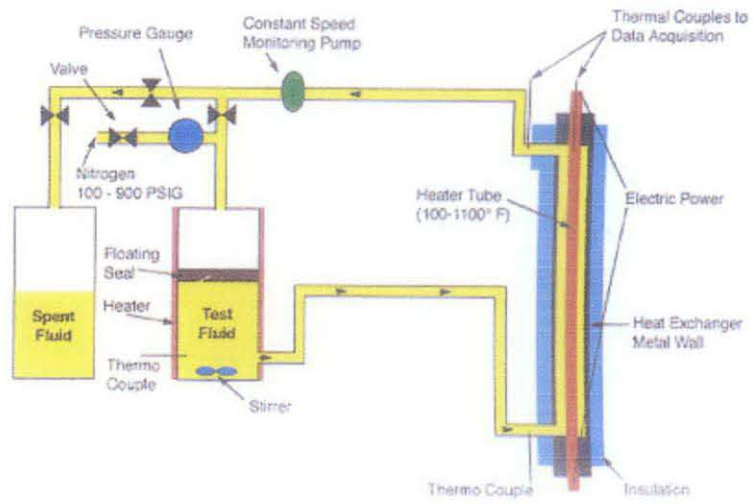


Figure 5: Schematic diagram of Hot Liquid Process Simulator 320 loop.

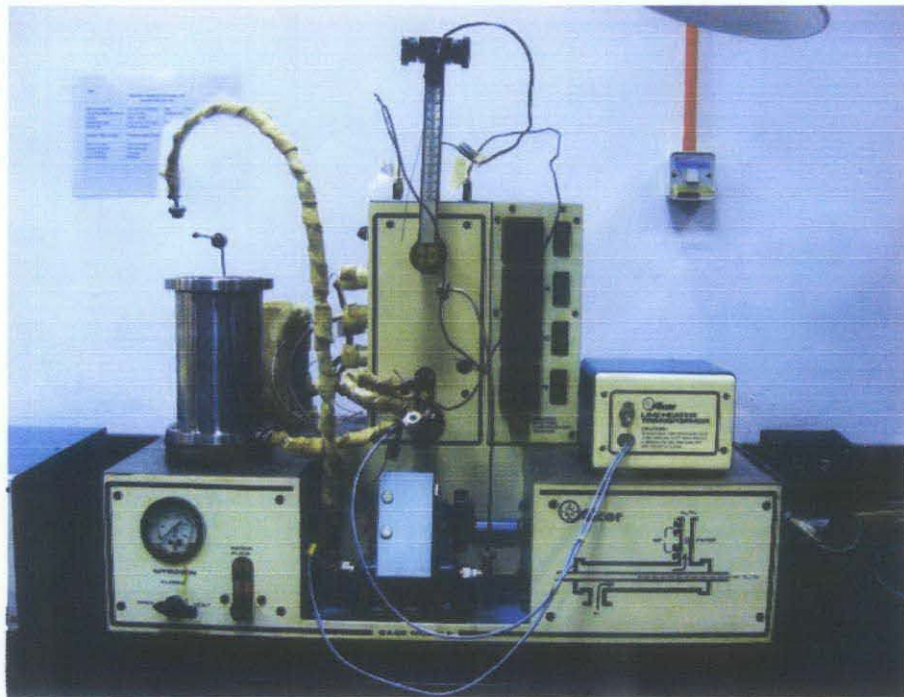


Figure 6: Experimental set-up of Hot Liquid Process Simulator 320.



Figure 7: Heater tube with clean surface before the experiment.

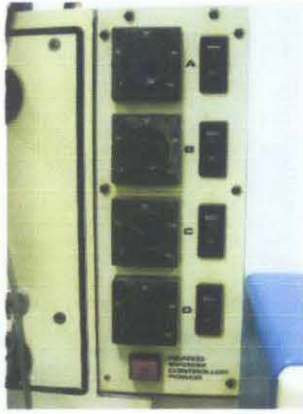


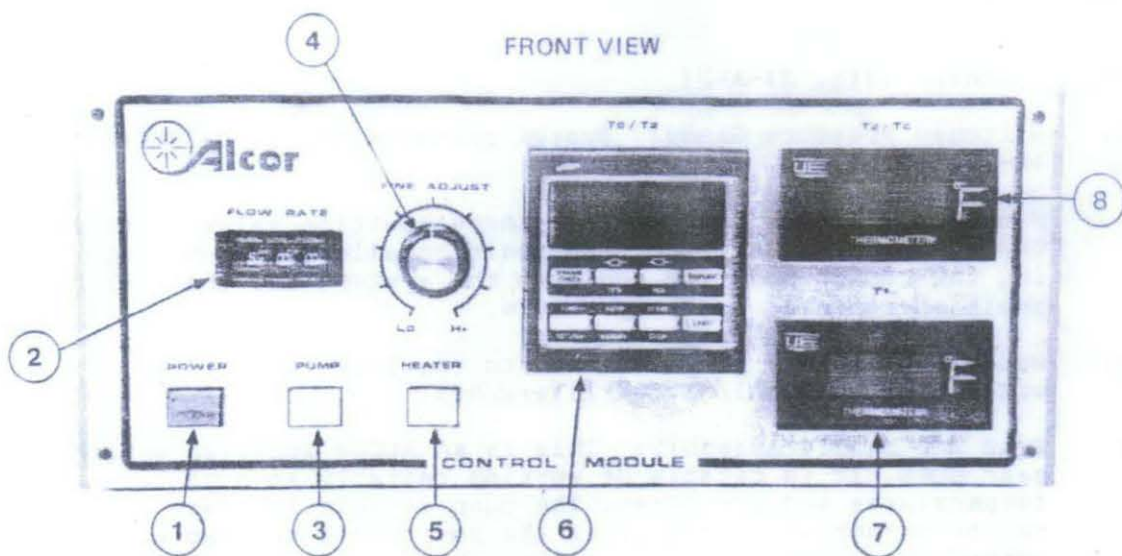
Figure 8: HLPS Heater System Controller.



Figure 9: Feed tank.

3.3.1 Specification of Apparatus

- Model: HLPS 320
- Base and Control System Specifications:
 - Sample Capacity: 500 ml
 - Heater Tube Temperature: 260°C
 - System Pressure: 6.9 MPa (1000 psi)
 - Flow Rate Possible: 3 ml/minute.
 - Base Size: 71 cm x 46 cm 47 cm height; 34 kg (75 lbs.) net.
 - Control Size: 43 cm x 31 cm x 18 cm height; 6.8 kg (15 lbs.) net.
- Heated System Specifications:
 - Four controllers: Pump, Reservoir and Lines
 - Temperature: pump (100°C), Reservoir (74°C), Lines (125-150°C)
 - Lines heated by external transformer circuit.
 - Three components of the heater system: (A) Reservoir heater jacket, (B) Pump heater jacket, and (C) Line heater system
- Installation needs:
 - Power: 115V/220V, 10 amp. max., 50/60 Hz.
 - Nitrogen: regulated 3.4 MPa (500 psi) maximum.
 - Water, cooling: 40 liter/hour (10 gal./hour) at 200-700 kPa (30-100 psi).
 - Drain: for cooling water discharge.



- | | |
|------------------------------------|--|
| 1. Power Switch | 7. Temperature Indicator, Fluid Inlet |
| 2. Flow Rate Control Pot. | 8. Temperature Indicator, Fluid Outlet/Heater Tube |
| 3. Pump Switch | 9. Base Module Interface Cable Socket |
| 4. Manual Control Fine Adjust Pot. | 10. Fuse |
| 5. Heater Switch | 11. External Power Connection |
| 6. Temperature Controller | 12. Thermocouple Connections |

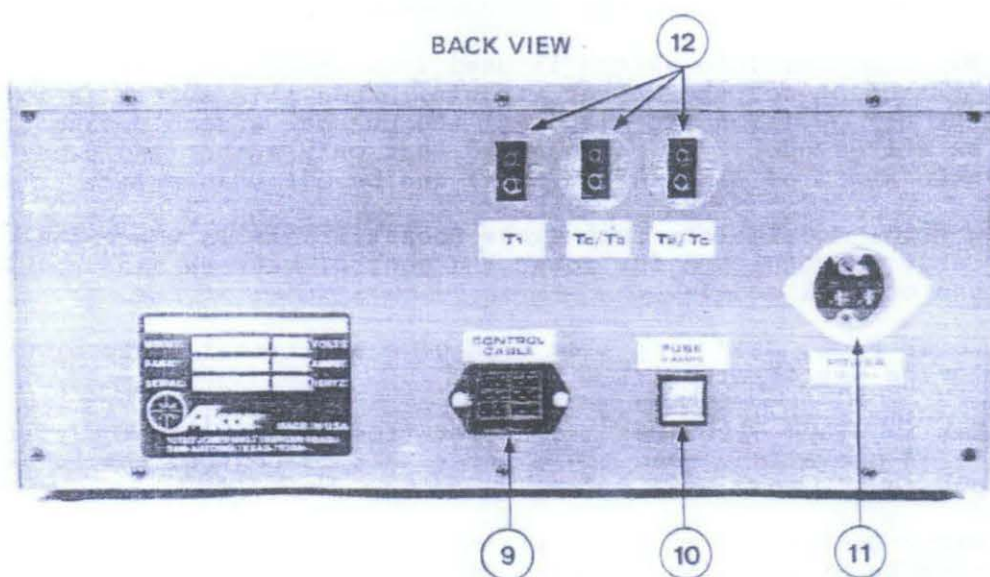


Figure 10: Basic Alcor's HLPS 320 System

3.4 OPERATING PROCEDURES

1. The heater tube thermocouple is lowered into the tube and set at 14 mm position on the long scale
2. The reservoir is opened and the piston, stir guard and stirrer are removed
3. The inlet line is attached to the outlet of the reservoir. The other end of this line is plugged in.
4. The stir guard and stirrer are placed back in the reservoir.
5. A sample of crude oil is poured into the reservoir.
6. The reservoir is placed on the base assembly and the stirrer speed is adjusted.
7. The piston is placed on the piston puller and lowered into the reservoir.
8. The cap is bolted in place.
9. The pressure inlet line is attached from the fitting on the surface of the base assembly to the fitting on the reservoir.
10. Each of the connecting lines is inspected to ensure there is a sound o-ring at each end.
11. All connections are assured to be hand tight.
12. The nitrogen pressure valve is opened slightly and a low pressure of 150kPa (25psi) is placed.
13. Finding there are no leaks, the pressure is raised to 3400 kPa (500 psig)
14. On Control Module, the pump control thumbpot is set to 300 and the pump is turned on.
15. The controller is set in non-programmed mode to 260°C. The Fine Adjust Pot is made sure to be centered.
16. The Heater is switched on and Start/Stop position is touched on controller to start the process of heating the sample.
17. When the unit is heat soaked (20-30 min), the controller is placed in manual by pressing the Auto/Manual button.
18. When the temperature will drift out or down from the set point, the Fine Adjust Pot is used to correct this.

19. Then, the heater tube thermocouple is moved up to 0, then down to 60 and back to 40 in increment of 10. The readings at each location are recorded in 5 minutes. (This step is repeated every 15 minutes).
20. The Fine Adjust Pot is centered to return to auto mode and the Auto/Manual button is pressed.
21. The Start/Stop button is pressed on the controller back in “hold” and its output is turned off. Then heater is switched off.
22. The time required for the system to cool down to a reasonable temperature is observed and then the pump is turned off.
23. Carefully, the nitrogen pressure valve is turned to vent.
24. The same test is performed except the unit for controlling outlet temperature is set by interchanging the fluid out thermocouple and the heater tube thermocouple.

3.5 EXPERIMENTAL PROCEDURES

3.5.1 Sample preparation

A magnetic stirrer was placed inside the empty feed tank. 500 ml of crude oil is pumped into a clean beaker. The crude oil was filtered and transferred to the feed tank containing the stirrer, which holds liquid at a maximum volume of 500 ml. The feed tank was sealed off. All connecting tubes to the feed tank were fastened. The heater tube was then fixed in place and connecting tubes were fastened.

3.5.2 Pre-heat up and pressurization

The feed tank was pressurized with N₂ to 3.4 bar. The pump was then started and water was circulated. The system was allowed to stay this way for 5 minutes. Settings were keyed in at the HLPS controller and the heater system was switched on. Set point temperature was input according to the temperature needed for an experiment. The experiments ranged in set point temperature from 220°C to 260°C.

3.5.3 HLPS power-up

After the set point temperatures were input into the controller, surface temperature and bulk temperature were reached in approximately 15 minutes. The probe was switched to an automatic feedback controller which maintained the temperature at set point. During the experiment, temperature was maintained $\pm 2^{\circ}\text{C}$ within the set point temperature.

3.5.4 Fouling runs and data recording

Experiments were carried out for 3 hours of continuous operation. Axial temperature, inlet temperature, outlet temperature, heater jacket temperature, pump temperature and line temperature were taken at an interval of 15 minutes. This data was then analyzed using an excel spreadsheet.

3.5.5 Shut down

When the fouling run is stopped, the heaters were switched off to allow fluid inside to cool down to room temperature by continuing the circulation. The system was cooled under nitrogen gas to avoid air entry into the system. Once cooled down to room temperature as indicated at the display, the nitrogen gas was vented from the system and the probe was switched off. Crude oil from the feed tank was drained and the feed tank was cleaned for washing run. The heater tube was removed with extra care to prevent deposits from getting scraped off the surface. The deposits were allowed to dry for at least 30 minutes before weighing the heater tube.

3.5.6 Washing run of HLPS

500 ml Toluene solution was poured into the feed tank which was then sealed. The same procedure was carried out for Toluene for set-up except without the heater. The circulation of Toluene was carried out for approximately 2 hours. Nitrogen gas was vented out from the system and then Toluene was drained from the system.

3.5 PROGRESS AND MILESTONES

WBS	Tasks	Start	End	Duration (Days)	Working Days	25-Jan-10	1-Feb-10	8-Feb-10	15-Feb-10	22-Feb-10	1-Mar-10	8-Mar-10	15-Mar-10	22-Mar-10	29-Mar-10	5-Apr-10	12-Apr-10	19-Apr-10	26-Apr-10
1	Briefing and Student Progress	1/27/10	1/27/10	1	1														
1.1	Project Work commences	2/01/10	2/14/10	14	10														
2	Progress Report submission	2/25/10	4/11/10	46	32														
2.1	Progress Report 1 submission	2/25/10	2/25/10	1	1														
2.2	Progress Report 1 marks	3/05/10	3/05/10	1	1														
2.3	Progress Report 2	4/09/10	4/09/10	1	1														

Table 3: Progress and Milestone of the Project

3.5 PROGRESS AND MILESTONES

WBS	Tasks	Start	End	Duration (Days)	Working Days	5-Apr-10	12-Apr-10	19-Apr-10	26-Apr-10	3-May-10	10-May-10	17-May-10	24-May-10	31-May-10	7-Jun-10
3	Poster Exhibition / Pre-EDX/ EDX	4/08/10	4/17/10	10	7	■	■								
3.1	Poster Exhibition	4/08/10	4/08/10	1	1	■									
3.2	EDX	4/14/10	4/15/10	2	2		■								
4	Submission of Final Report	4/30/10	4/30/10	1	1				■						
5	Final Oral Presentation	5/24/10	6/06/10	14	10								■	■	
6	Submission of Hard Bound Copies	6/04/10	6/18/10	14	10									■	■

Table 4: Progress and Milestone of the Project (continued)

CHAPTER 4

RESULTS AND DISCUSSION

4.1 RESULTS

For assessment of fouling characteristics of a Malaysian crude oil, 6 experiments have been conducted at constant pressure of 3.4 MPa using HLPS equipment. The crude oil was kept running for a duration of 3 hours and data was recorded every 15 minutes. At the end of the experiments, fouled heater tube (probe) showed black deposits at the heated section.



Figure 11: Picture of a fouled probe after the experiment

A sample calculation at $T_b=100^\circ\text{C}$, $T_s=260^\circ\text{C}$ at 90 minutes is shown. For other data, the same calculation steps are used in order to get fouling resistance. The first step to analyze the fouling data is by calculating the average temperature driving force using the following equation:

$$\Delta T_m = \frac{\sum_{i=3}^{11} [T_s(z)_i - T_b(z)_i]}{6} \quad [5]$$

$$\Delta T_m = \frac{650.60}{6}$$

$$\Delta T_m = 108.43$$

Here the temperature driving force is calculated for every 15 minutes for the duration of 3 hours. Temperature profile reading is taken at 8 points starting 0mm to 60mm for every set of experiment. For the purpose of calculating average temperature driving force, only six temperature profiles are used, from 10mm to 50mm. As the bulk fluid increases with time, the average temperature also increases.

Heat capacity is estimated using the formulation below which is based on the crude oil properties:

$$C_p = 3.746897 \times T_b + 775.44126 \quad [6]$$

$$C_p = 3.746897 \times 411.15 + 775.44126$$

$$C_p = 2315.978 \frac{J}{kg.K}$$

whereby T_b is taken as average bulk temperature.

The overall heat transfer coefficient can then be determined using the sensible heat gain of the fluid:

$$U(t) = \frac{mC_p(T_{b,z=50mm} - T_{b,z=10mm})}{A \times \Delta T_m} \quad [7]$$

$$U(t) = \frac{(3.74 \times 10^{-5})(2315.98)(450.15 - 372.15)}{0.000588 \times 108.43}$$

$$= 70.61 \frac{J}{m^2 \cdot s}$$

- where m = mass flowrate (kg/s)
 C_p = heat capacity (J/Kg.K)
 A = heat transfer surface area (m²)
 ΔT_m = average temperature driving force

Once the overall heat transfer coefficient has been calculated, fouling resistance R_f can be obtained using equation [8] .

$$R_f = \frac{1}{U(t)} - \frac{1}{U_i} \quad [8]$$

$$R_f = \frac{1}{114.2398} - \frac{1}{118.6758} = 0.000327 \frac{m^2 \cdot K}{W \cdot min}$$

The calculations will be repeated for bulk temperatures of 70°C, 80°C and surface temperatures 220°C and 260°C.

Three experiments were carried out at a constant surface temperature of 260°C and varying bulk temperatures at 70°C, 80°C and 100°C. At bulk temperature of 70°C, there was a short initial spike in fouling rate in the first 15 minutes. Initial fouling rate is 9.77E-06 m²K/W.min.

At bulk temperature of 80°C, there was an induction period in the first 15 minutes. Rapid fouling occurred afterwards in the first 60 minutes, making the initial fouling rate $3.49\text{E-}05 \text{ m}^2\text{K/W.min}$ which is 72% higher than initial fouling rate at 70°C.

At bulk temperature 100°C, the initial fouling rate is $5.724\text{E-}05 \text{ m}^2\text{K/W.min}$ which makes it the highest rate compared to other bulk temperatures.

Although there is a considerable scatter, the crude oil operating at the highest operating bulk temperature has the highest initial fouling rate, while the lowest operating bulk temperature has the lowest initial fouling rate. With a fixed surface temperature, fouling rates increases considerably with bulk temperature.

Another set of experiment was carried out and results of the experiments are plotted in the graph below.

Experiments at fixed bulk temperature of 80°C and at varying surface temperatures from 220°C to 260°C was carried out. At surface temperature of 220°C, initial fouling rate is $2.19\text{E-}05 \text{ m}^2\text{K/W.min}$. This is obtained by finding the slope of the initial fouling process. At 75 minutes, the fouling rate became constant.

At surface temperature of 240°C, the initial fouling rate is $3.40\text{E-}05 \text{ m}^2\text{K/W.min}$ which makes it 1.5 times higher than at surface temperature of 220°C. Initial fouling rate at surface temperature of 260°C is $3.49\text{E-}05 \text{ m}^2\text{K/W.min}$.

At all surface temperatures, the fouling resistance, R_f shoots up high in the beginning but began to level out after a certain period. This shows that fouling process is accelerated in the beginning, and then slows down when the process hits a time where fouling occur less.

4.2 EFFECT OF BULK TEMPERATURE

Three experiments were carried out at a constant surface temperature of 220°C, 240°C and 260°C for bulk temperatures of 70°C, 80°C and 100°C. Figure 12 shows the fouling trend.

From calculations based on the experimental results, it is observed that an obvious trend can be seen for bulk temperatures 70°C, 80°C and 100°C. Fouling rates increases sharply with initial bulk temperature. The rates were 6 times faster at an increased bulk temperature of 30°C.

As the bulk temperature increases from 70°C to 100°C, fouling rates also increases accordingly whereby the order of increasing fouling rate is 70°C < 80°C < 100°C. The increase of fouling rates due to changes in bulk temperature is because of the salvation of precursors in the crude. A summary of initial fouling rates is shown in table 5 below. The trend clearly points towards an increase in initial fouling rates as the bulk temperature increases.

Table 5: Initial fouling rates at constant $T_s= 260^\circ\text{C}$ and bulk temperatures 70°C, 80°C and 100°C.

Bulk temperature (°C)	Initial fouling rates ($\text{m}^2.\text{K}/\text{W}.\text{min}$)
70	9.773E-06
80	3.492E-05
100	5.724E-05

A comparison of fouling resistance at surface temperature of 260°C and bulk temperatures of 70°C, 80°C and 100°C is shown in the graph below:

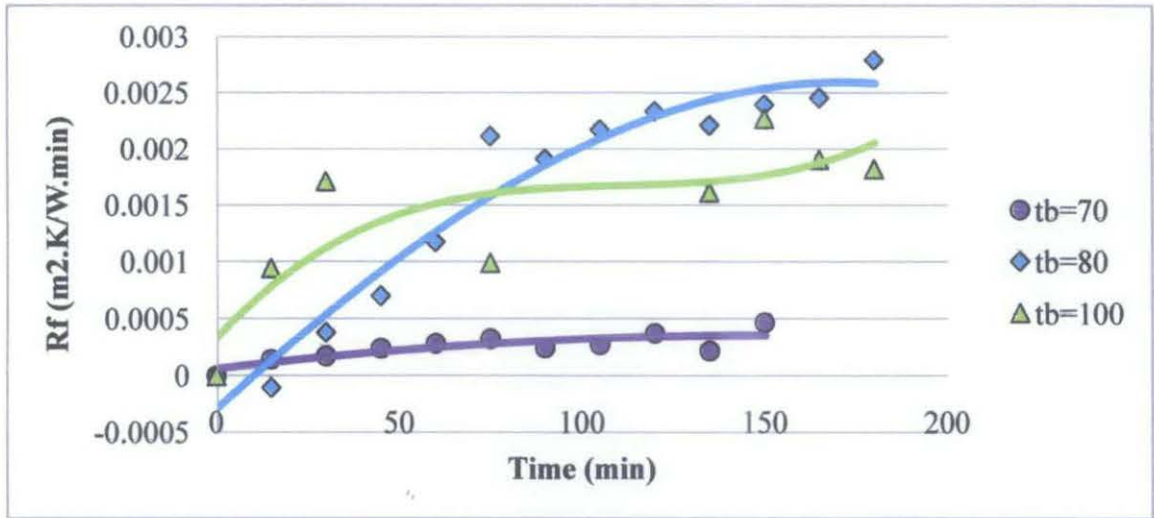


Figure 12: Comparison of fouling rates at bulk temperatures 70°C, 80°C and 100°C with $T_s=260^\circ\text{C}$

After 150 minutes, fouling process has reached a steady state for bulk temperature 80°C. At bulk temperature 100°C, steady state is reached at 75 minutes which is faster than 80°C. This shows that precursors to fouling has been used up rapidly during the initial fouling process and subsequently reaching steady state faster at bulk temperature 100°C compared to bulk temperature 80°C.

Using the correlation that is shown below, the experimental results are then fitted with predicted results. The Ebert-Panchal correlation used:

$$dR_f/dt = aRe^{-b} \exp(-E/RT_f) - gt_w$$

The calculated results are tabulated below. Table 6 shows predicted fouling rates which is derived from the calculation using the Ebert Panchal correlation. Both results show similarity with little deviation. Fitting results showed an 89% match between experimental and predicted values.

Table 6: Experimental and predicted initial fouling rates for constant $T_s=260^\circ\text{C}$

T_b °C	dRf/dt predicted	dRf/dt experiment	
	m2K/Whr	m2K/Wmin	m2K/Whr
70	1.05E-03	9.77E-06	5.864E-04
80	1.61E-03	3.49E-05	2.095E-03
100	3.44E-03	5.72E-05	3.435E-03

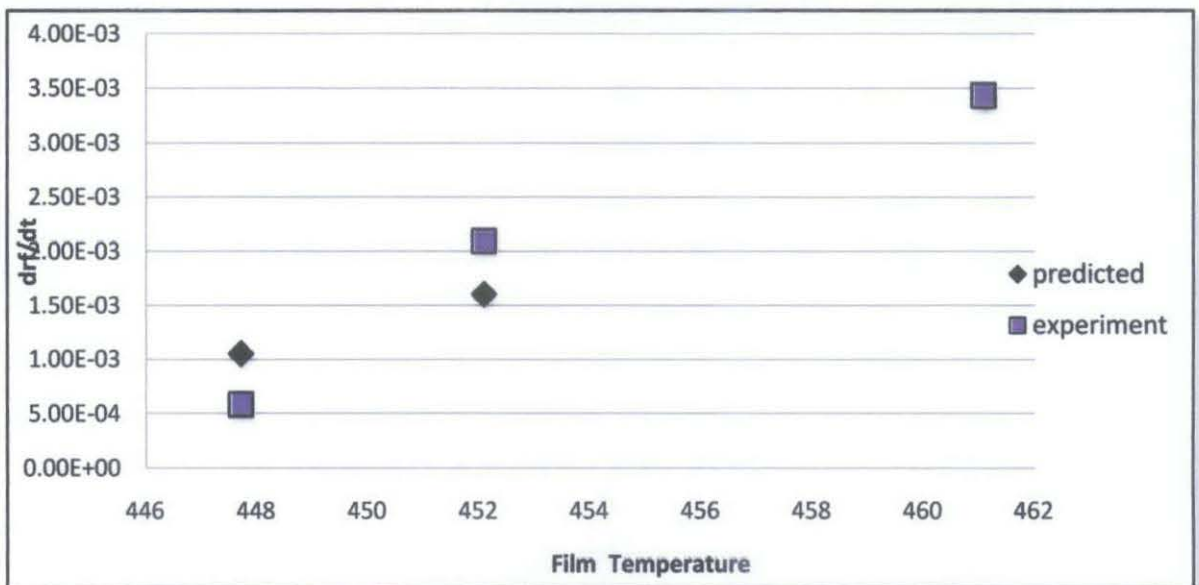


Figure 13: Experimental results at constant $T_s=260^\circ\text{C}$ fitted to Ebert-Panchal model of fouling threshold

Table 7: Summary of results at varying bulk temperatures at $T_s=260^\circ\text{C}$

Min	$T_b = 70^\circ\text{C}$				$T_b = 80^\circ\text{C}$				$T_b = 100^\circ\text{C}$			
	T1 (°K)	T2(°K)	T_{bm}	U_t	T1(°K)	T2(°K)	T_{bm}	U_t	T1(°K)	T2(°K)	T_{bm}	U_t
0	343.15	474.15	408.65	118.6758	353.15	456.15	404.65	90.2866	373.15	459.15	416.15	79.96361
15	343.15	473.15	408.15	116.6465	352.15	457.15	404.65	91.12433	373.15	453.15	413.15	74.33113
30	343.15	472.15	407.65	116.2358	352.15	454.15	403.15	87.25736	374.15	450.15	412.15	70.30879
45	343.15	472.15	407.65	115.3523	352.15	452.15	402.15	84.86142	373.15	451.15	412.15	72.76073
60	343.15	471.15	407.15	114.7622	353.15	449.15	401.15	81.60741	373.15	452.15	412.65	74.07412
75	343.15	471.15	407.15	114.2398	353.15	445.15	399.15	75.77931	372.15	450.15	411.15	70.61055
90	343.15	471.15	407.15	115.2895	353.15	445.15	399.15	76.96888	372.15	454.15	413.15	72.9979
105	343.15	471.15	407.15	114.9375	353.15	445.15	399.15	75.46123	371.15	451.15	411.15	73.81277
120	343.15	470.15	406.65	113.6478	354.15	445.15	399.65	74.53811	374.15	451.15	412.65	70.8166
135	344.15	469.15	406.65	115.6845	353.15	445.15	399.15	75.25066	374.15	448.15	411.15	67.66203
150	344.15	470.15	407.15	112.4093	354.15	445.15	399.65	74.22704	372.15	448.15	410.15	69.38656
165	344.15	471.15	407.65	109.1341	354.15	444.15	399.15	73.89659	372.15	449.15	410.65	69.78566
180	344.15	472.15	408.15	105.8589	354.15	444.15	398.15	72.09671	372.15	448.15	412.55	69.6642

4.3 EFFECT OF SURFACE TEMPERATURE

Three sets of experiments were carried out for constant bulk temperature of 70°C, 80°C and 100°C with initial surface temperatures of 220°C, 240°C and 260°C. The fouling resistance against time plot shows a trend that when the surface temperature increases, this results in an increase in initial fouling rates. At different bulk temperatures, an increase in surface temperature shows same results.

Initial fouling rates are taken from the beginning slope of the graph, indicating where solid particles start to deposit on the surface of the heater tube. The first portion of the graph is taken and given a linear trend line. This gives the value of initial fouling rates.

Table 8: Initial fouling rates at constant bulk temperature of 70°C

Surface temperature (°C)	Initial fouling rates (m ² .K/W.min)
220	8.51E-06
240	9.50E-06
260	9.773E-06

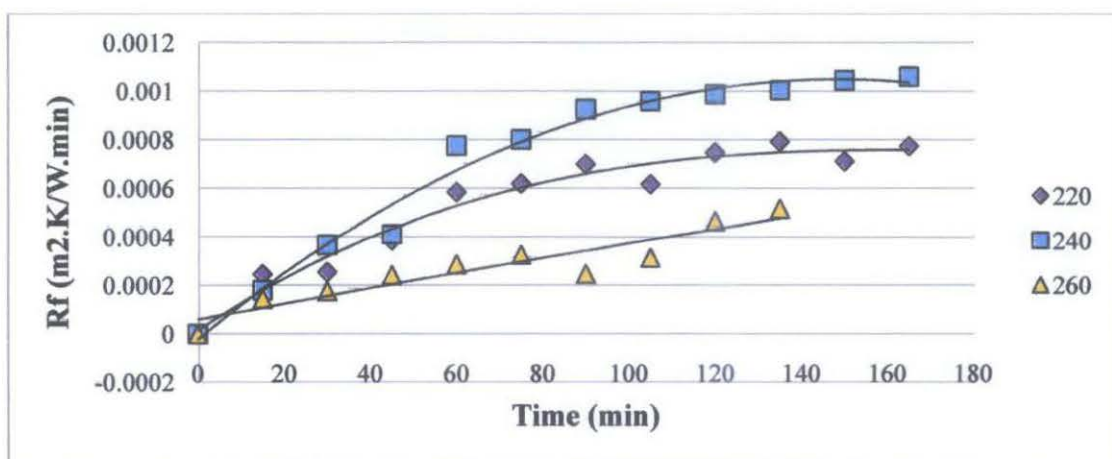


Figure 14: Fouling resistance plotted against time at $T_b=70^\circ\text{C}$ for surface temperatures of 220°C, 240°C, and 260°C

Table 9: Initial fouling rates at constant bulk temperature of 80°C

Surface temperature (°C)	Initial fouling rates (m ² .K/W.min)
220	1.85E-05
240	3.02E-05
260	3.492E-05

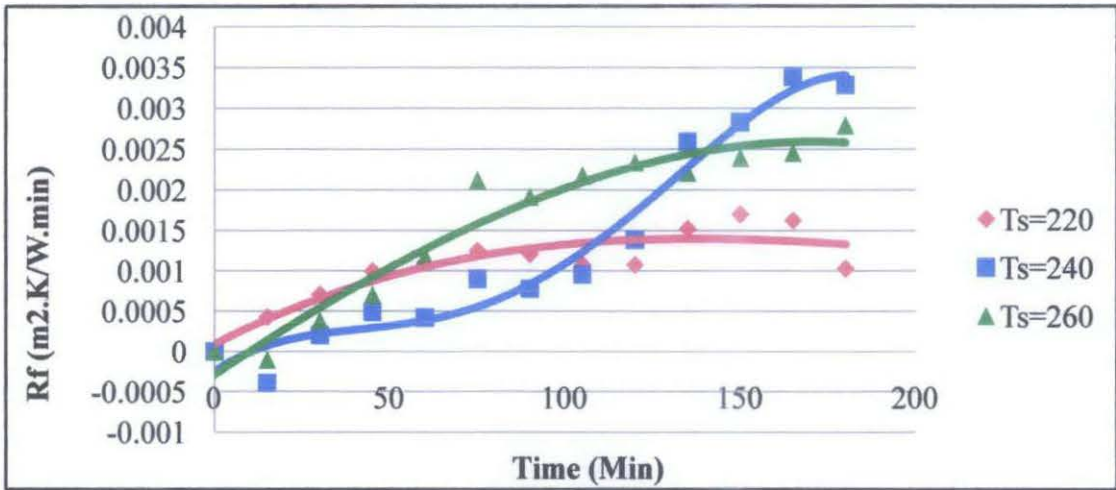


Figure 15: Fouling resistance plotted against time at $T_b=80^\circ\text{C}$ for surface temperatures of 220°C, 240°C, and 260°C

Table 10: Initial fouling rates at constant bulk temperature of 100°C

Surface temperature (°C)	Initial fouling rates (m ² .K/W.min)
220	1.14E-05
240	2.03E-05
260	5.724E-05

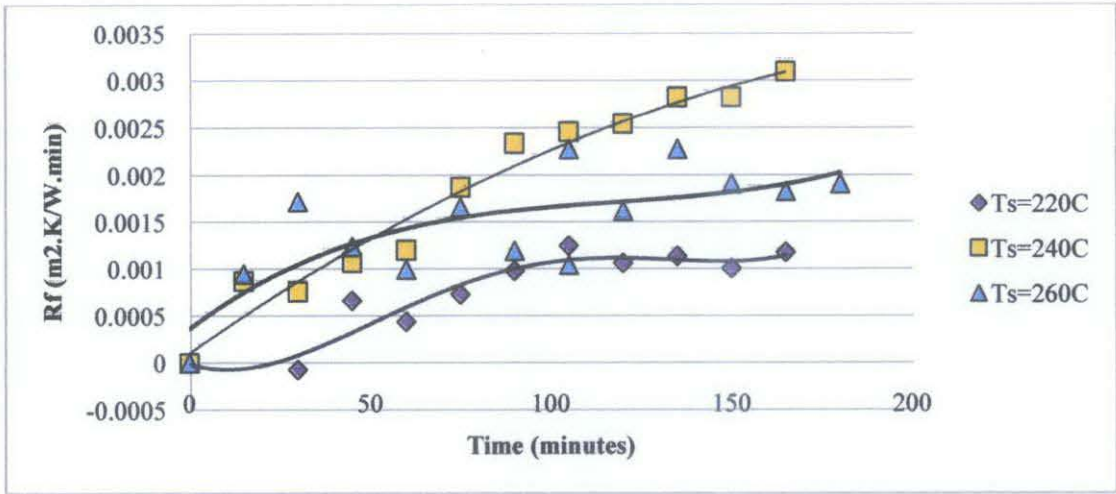


Figure 16: Fouling resistance plotted against time at $T_b=100^\circ\text{C}$ for surface temperatures of 220°C , 240°C , and 260°C

Figure 14-16 shows fouling resistance at constant bulk temperatures of 70°C , 80°C and 100°C . From this plot, it can be said that at surface temperature of 260°C , fouling deposition will occur more rapidly than at a temperature of 220°C . The reasons for this are unclear, but past studies had linked fouling at higher temperatures with chemical reaction fouling which is an extremely complex process which could involve several mechanisms.

Even at higher bulk temperatures, such as 100°C , initial fouling rates showed the same pattern. Below in figure 15, the results of the experiment showed that at bulk temperature of 100°C , the fouling deposition occur more rapidly at surface temperature of 260°C compared to 220°C .

To further analyze the experimental results, fouling rates are plotted on a semi log Arrhenius graph versus inverse of film temperature. Film temperature in this case takes into consideration average of bulk temperature and surface temperature. The film temperature gives equal weightage to bulk temperature and surface temperature. This can be seen in the formula for film temperature below:

$$T_f = T_{b,average} + 0.55*(T_s - T_{b,average})$$

After attaining film temperature, the inverse of film temperature is taken to be plotted against the log of initial fouling rates in an Arrhenius plot to find the activation energy. The log of fouling rates and inverse of film temperatures are tabulated below:

Table 11: Log values of initial fouling rates at constant $T_b=80^\circ\text{C}$

T_s ($^\circ\text{C}$)	Initial fouling rates ($\text{m}^2\cdot\text{K}/\text{W}\cdot\text{min}$)	$\ln dRf/dt$	T_f ($^\circ\text{K}$)	$1/T_f$
220	2.19E-05	-10.72902392	445.5192308	0.002244572
240	3.40E-05	-10.28915003	459.6	0.002175805
260	3.49E-05	-10.26302373	473.7090909	0.002111



Figure 17: Arrhenius plot of fouling rate versus inverse film temperature at constant $T_b=80^\circ\text{C}$

At bulk temperature 80°C , the slope is -3520 which is shown in figure 18. R is given as $0.008314 \text{ kJ/mol}\cdot\text{K}$. By multiplying the slope with R , activation energy is found to be 29.27 kJ/mol . Comparing this value to Srivinasan and Watkinson's (2003) result, it can be assumed that chemical reaction fouling is the major fouling mechanism in this case.

Table 12: Experimental and predicted initial fouling rates at constant bulk temperature $T_b=80^\circ\text{C}$

T_s °C	dRf/dt predicted	dRf/dt experiment	
	$\text{m}^2\text{K}/\text{Whr}$	$\text{m}^2\text{K}/\text{Wmin}$	$\text{m}^2\text{K}/\text{Whr}$
220	1.34E-03	2.19E-05	1.314E-03
240	1.72E-03	2.94E-05	1.764E-03
260	2.12E-03	3.49E-05	2.094E-03

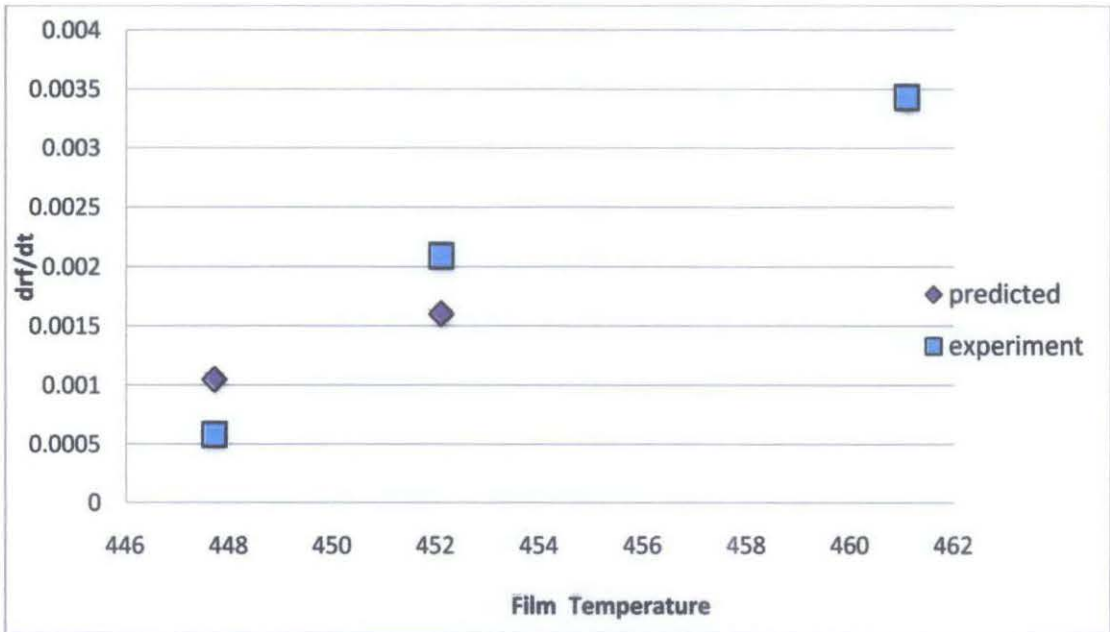


Figure 18: Experimental results at constant $T_b=80^\circ\text{C}$ fitted to Ebert-Panchal model of fouling threshold.

Table 13 shows the results obtained from Ebert-Panchal model and experimental results. Compared to Ebert-Panchal model fitting at varying bulk temperatures, results at varying surface temperatures gave a better fit of 99%. This shows that the Ebert-Panchal model is more suitable to be used for experiments using constant bulk temperature and varying surface temperatures.

Table 13: Summary of results at varying surface temperatures at $T_b=70^\circ\text{C}$

min	$T_s = 220^\circ\text{C}$				$T_s = 240^\circ\text{C}$				$T_s = 260^\circ\text{C}$			
	T1($^\circ\text{K}$)	T2($^\circ\text{K}$)	T_{bm}	U_t	T1($^\circ\text{K}$)	T2($^\circ\text{K}$)	T_{bm}	U_t	T1 ($^\circ\text{K}$)	T2 ($^\circ\text{K}$)	T_{bm}	U_t
0	343.15	446.15	394.65	117.4228	343.15	470.15	406.65	136.2502	343.15	474.15	408.65	118.6758
15	342.15	446.15	394.15	114.1201	344.15	470.15	407.15	132.9867	343.15	473.15	408.15	116.6465
30	343.15	445.15	394.15	114.0069	342.15	470.15	406.15	129.7526	343.15	472.15	407.65	116.2358
45	343.15	443.15	393.15	112.3094	343.15	469.15	406.15	129.0005	343.15	472.15	407.65	115.3523
60	343.15	442.15	392.65	109.8678	343.15	468.15	405.65	123.2032	343.15	471.15	407.15	114.7622
75	343.15	442.15	392.65	109.4523	344.15	468.15	406.15	122.8314	343.15	471.15	407.15	114.2398
90	343.15	441.15	392.15	108.5007	344.15	467.15	405.65	120.975	343.15	471.15	407.15	115.2895
105	342.15	440.15	391.15	109.4896	342.15	466.15	404.15	120.5032	343.15	471.15	407.15	114.9375
120	343.15	440.15	391.65	107.956	343.15	465.15	404.15	118.5073	343.15	470.15	406.65	113.6478
135	342.15	440.15	391.15	107.4351	342.15	464.15	403.15	117.1054	344.15	469.15	406.65	115.6845
150	343.15	440.15	391.65	108.3688	343.15	464.15	403.65	117.2932	344.15	470.15	407.15	112.4093
165	342.15	440.15	391.15	107.6371	342.15	464.15	403.15	116.3446	343.15	474.15	408.65	118.6758
180	343.15	440.15	391.65	117.4228	342.15	464.15	403.15	136.2502	343.15	473.15	408.15	116.6465

Table 14: Summary of results at varying surface temperatures at $T_b=80^\circ\text{C}$

Min	$T_s = 220^\circ\text{C}$				$T_s = 240^\circ\text{C}$				$T_s = 260^\circ\text{C}$			
	T1($^\circ\text{K}$)	T2($^\circ\text{K}$)	T_{bm}	U_t	T1($^\circ\text{K}$)	T2($^\circ\text{K}$)	T_{bm}	U_t	T1 ($^\circ\text{K}$)	T2 ($^\circ\text{K}$)	T_{bm}	U_t
0	353.15	426.15	389.65	75.9372	352.15	439.15	395.65	80.6601	353.15	456.15	404.65	90.2866
15	353.15	424.15	388.65	73.5263	353.15	442.15	397.65	83.2786	352.15	457.15	404.65	91.1243
30	352.15	422.15	387.15	72.0403	352.15	440.15	396.15	79.359	352.15	454.15	403.15	87.2574
45	353.15	421.15	387.15	70.5714	352.15	439.15	395.65	77.5881	352.15	452.15	402.15	84.8614
60	353.15	421.15	387.15	70.0726	353.15	439.15	396.15	78.0039	353.15	449.15	401.15	81.6074
75	353.15	421.15	387.15	69.3375	353.15	438.15	395.65	75.201	353.15	445.15	399.15	75.7793
90	354.15	421.15	387.65	69.5332	353.15	440.15	396.65	75.8868	353.15	445.15	399.15	76.9689
105	353.15	421.15	387.15	70.1967	354.15	440.15	397.15	74.9039	353.15	445.15	399.15	75.4612
120	353.15	421.15	387.15	70.1967	353.15	432.15	392.65	72.5659	354.15	445.15	399.65	74.5381
135	353.15	420.15	386.65	68.0482	354.15	428.15	391.15	66.7053	353.15	445.15	399.15	75.2507
150	353.15	420.15	386.65	67.2284	353.15	427.15	390.15	65.6624	354.15	445.15	399.65	74.227
165	353.15	420.15	386.65	67.5773	353.15	425.15	389.15	63.3519	354.15	444.15	399.15	73.8966
180	352.15	420.15	386.15	70.4134	354.15	426.15	390.15	63.765	354.15	442.15	398.15	72.0967

Table 15: Summary of results at varying surface temperatures at $T_b=100^\circ\text{C}$

min	$T_s = 220^\circ\text{C}$				$T_s = 240^\circ\text{C}$				$T_s = 260^\circ\text{C}$			
	T1(°K)	T2(°K)	T_{bm}	U_t	T1(°K)	T2(°K)	T_{bm}	U_t	T1 (°K)	T2 (°K)	T_{bm}	U_t
0	374.15	443.15	408.65	104.1597	353.15	426.15	389.65	75.93721	373.15	459.15	416.15	79.96361
15	372.15	446.15	409.15	98.72665	353.15	424.15	388.65	73.5263	373.15	453.15	413.15	74.33113
30	373.15	447.15	410.15	104.9484	352.15	422.15	387.15	72.04026	374.15	450.15	412.15	70.30879
45	373.15	447.15	410.15	97.43756	353.15	421.15	387.15	70.57144	373.15	451.15	412.15	72.76073
60	373.15	445.15	409.15	99.61106	353.15	421.15	387.15	70.07265	373.15	452.15	412.65	74.07412
75	373.15	444.15	408.65	96.81358	353.15	421.15	387.15	69.33753	372.15	450.15	411.15	70.61055
90	373.15	443.15	408.15	94.52687	354.15	421.15	387.65	69.53317	372.15	454.15	413.15	72.9979
105	373.15	443.15	408.15	92.19897	353.15	421.15	387.15	70.19668	371.15	451.15	411.15	73.81277
120	374.15	443.15	408.65	93.81108	353.15	421.15	387.15	70.19668	374.15	451.15	412.65	70.8166
135	374.15	443.15	408.65	93.16529	353.15	420.15	386.65	68.04821	374.15	448.15	411.15	67.66203
150	373.15	443.15	408.15	94.3104	353.15	420.15	386.65	67.22845	372.15	448.15	410.15	69.38656
165	373.15	443.15	408.15	92.8224	353.15	420.15	386.65	67.57734	372.15	449.15	410.65	69.78566
180	374.15	443.15	408.65	104.1597	352.15	420.15	386.15	70.41336	373.15	459.15	416.15	79.96361

CHAPTER 5

CONCLUSION AND RECOMMENDATIONS

5.1 CONCLUSIONS

Two parts of experiments were conducted at constant velocity, using the same crude oil. The first set of experiment was conducted at constant surface temperature of 260°C and varying bulk temperatures 70°C-100°C. The second set of experiment was conducted at fixed bulk temperature of 80°C and at varying surface temperatures of 220°C-260°C. Both sets of experiments were conducted in the HLPS 320 equipment with nitrogen gas at 3400psia as inert. The HLPS equipment was kept running up to 3 hours for each experiment. Bulk temperature, surface temperature and axial temperature profile data was monitored every 15 minutes.

From the experimental results, it is apparent that **fouling rate increases with the increasing bulk temperatures**. Low temperatures, on the other hand seem to reduce fouling effects on the equipment. Fouling rates can be calculated by using sensible heat gain of the crude oil and heat capacity can be estimated with a correlation using bulk temperature.

From the second set of experiment, it can be concluded that **fouling rates increase with increasing surface temperature**. Arrhenius curve was plotted which gave the **activation energy of 29.27 kJ/mol**. The activation energy indicates chemical reaction fouling.

5.2 RECOMMENDATIONS

Further experimental work needs to be done to explain in detail the effects of varying surface temperature and bulk temperature on Malaysian crude oil fouling. This can be done by testing on a higher and wider range of bulk temperatures and surface temperatures.

This particular experiment only tested fouling on one type of crude oil. Other Malaysian crude oils can also be tested for fouling effects, as well as blends. System operating variables such as pressure, flow rate or velocity can also be experimented upon.

There were a few limitations to the current HLPS system. The same experiment could be implemented on the latest HLPS system. There are also other types of system that gauges fouling deposition such as HTRI and PRFU probes.

As a step further to reduce error in results, an experiment should be conducted at least two times. The average value can then be taken as result. This can assure more accurate results and reduce experimental errors.

REFERENCES

- Bott, T. (1995). *Fouling of Heat Exchangers*. The Netherlands: Elsevier Science B.V.
- D.I. Wilson, G. P. (2005). Ten Years of Ebert, Panchal and the Threshold Fouling Concept. *Symposium Series, Volume RP2* , 1-3.
- Isogai, S. N. (2004). Analysis and Steps to Mitigate Heat Exchanger Fouling in an Aromatics Plant. *ECI Conference on Heat Exchanger Fouling and Cleaning: Fundamentals and Applications*. New Mexico, USA.
- Lambourn, G. D. (1983). *Fouling in Crude Oil Preheat Trains in Heat Exchangers Theory and Practice*. New York: Hemisphere Publishing.
- Müller-Steinhagen, H. (2000). *Heat Exchanger Fouling: Mitigation and Cleaning Techniques*. Warwickshire, UK: Institution of Chemical Engineers.
- Nasr, M. G. (2005). Modeling of crude oil fouling in preheat exchangers of refinery distillation units. *Applied Thermal Engineering* .
- Saleh, Z. S. (2004). Fouling Characteristics of a Light Australian Crude Oil. *ECI Conference on Heat Exchanger Fouling and Cleaning: Fundamentals and Applications*, (p. 1). New Mexico, USA.
- Scarborough, C. C. (1979). Coking of Crude Oil at High Heat Flux Levels. *Chem. Eng. Proc.*
- Watkinson, A. (2004). Comparison of Crude Oil Fouling Using Two Different Probes. *ECI Conference on Heat Exchanger Fouling and Cleaning: Fundamentals and Applications*. New Mexico, USA.
- Watkinson, A. W. (1997). Chemical Reaction Fouling: A Review.
- Yeap, B. L. (2004). Mitigation of Crude Oil Refinery Heat Exchanger. *Chemical Engineering Research and Design* , 2-4.

APPENDIX

FOULING IN HEAT EXCHANGERS



Tube side fouling

(Source: Imperial College London.

<http://www3.imperial.ac.uk/crudeoilfouling/foulingpics>)



Shell side fouling

(Source: Imperial College London.

<http://www3.imperial.ac.uk/crudeoilfouling/foulingpics>)

EXPERIMENTAL APPARATUS

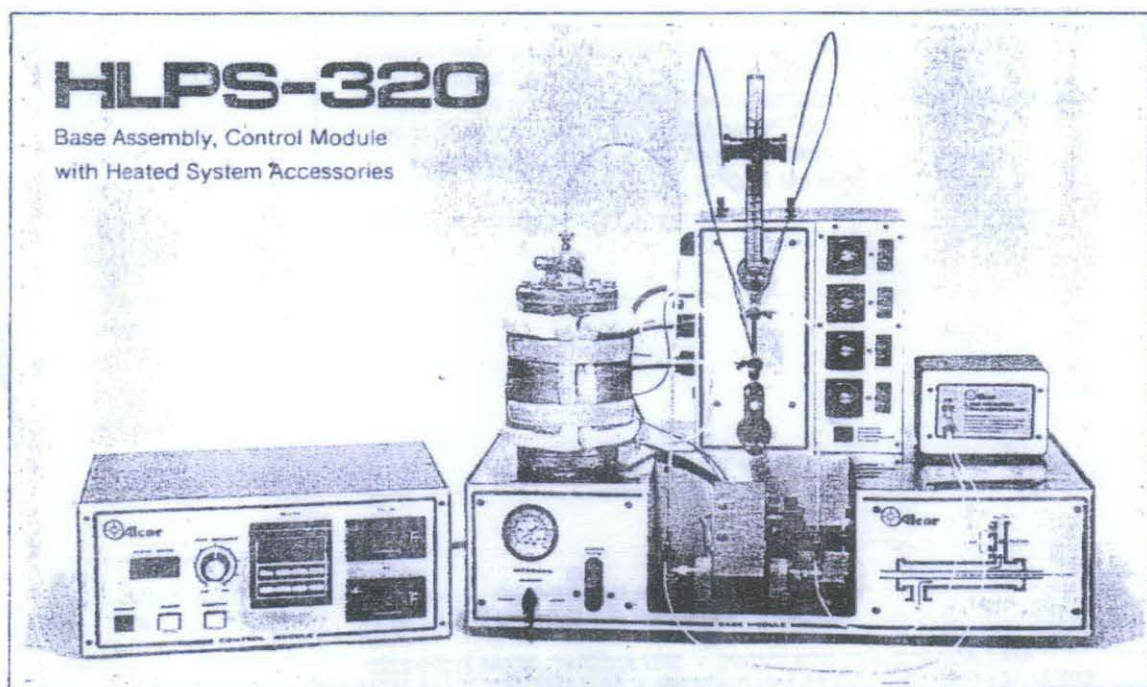
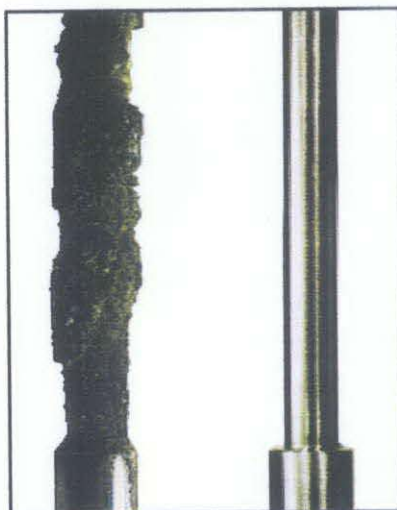


Diagram of Experimental Setup HLPS 320



Heater tube before fouling experiment (right) and after.

EXPERIMENTAL RAW DATA

Duration (min)	T1 (°C)	T2 (°C)	Tc (°C) Tube Profile (mm)								
14			0	10	20	30	38	40	50	60	
15	100	186	189	225	251	263	265	263	237	178	
15	100	180	188	222	248	260	261	260	234	180	
15	101	177	186	219	246	261	261	260	234	176	
15	100	178	183	218	245	259	260	260	234	178	
15	100	179	185	220	245	261	260	259	231	175	
15	99	177	188	225	248	262	260	261	233	174	
15	99	181	195	228	256	268	260	265	236	176	
15	98	178	194	227	248	261	261	258	222	171	
15	101	178	195	226	248	261	261	260	232	170	
15	101	175	193	225	250	262	260	259	226	169	
15	99	175	191	224	250	262	260	259	222	166	
15	99	176	196	227	252	263	260	259	224	165	

Experimental results at $T_s = 260^\circ\text{C}$ and $T_b = 100^\circ\text{C}$

EXPERIMENTAL RAW DATA

Duration (min)	T1 (°C)	T2 (°C)	Tc (°C) Tube Profile (mm)							
13			0	10	20	30	38	40	50	60
15	80	183	186	220	243	255	261	259	235	183
15	79	184	188	223	245	256	261	259	236	184
15	79	181	187	222	245	256	261	260	236	180
15	79	179	184	220	245	256	261	260	237	180
15	80	176	184	218	244	255	261	260	233	178
15	80	172	186	220	246	259	261	260	234	175
15	80	172	185	219	244	256	260	259	231	176
15	80	172	186	222	245	259	261	261	235	178
15	81	172	188	224	249	260	261	260	233	179
15	80	172	189	224	249	259	260	259	234	176
15	81	172	190	226	249	261	261	260	233	175
15	81	171	188	222	248	259	261	260	232	175
15	81	169	188	223	247	258	260	258	231	173

Experimental results at $T_s=260^\circ\text{C}$ and $T_b=80^\circ\text{C}$

EXPERIMENTAL RAW DATA

Duration (min)	T1 (°C)	T2 (°C)	Tc (°C) Tube Profile (mm)								
10			0	10	20	30	38	40	50	60	
15	70	201	183	221	248	260	261	260	230	172	
15	70	200	184	223	251	262	260	259	228	168	
15	70	199	189	222	248	260	260	258	229	171	
15	70	199	183	220	250	262	261	258	231	173	
15	70	198	183	220	249	259	261	259	229	170	
15	70	198	186	221	248	262	260	260	229	171	
15	70	198	187	222	246	259	261	258	228	170	
15	70	198	188	218	246	259	261	258	234	168	
15	70	197	188	222	246	260	261	257	229	171	
15	71	196	185	215	239	254	258	259	228	168	
15	71	197	193	221	250	261	260	259	229	172	

Experimental results at Ts=260°C and Tb=70°C

EXPERIMENTAL RAW DATA

Duration (min)	T1 (°C)	T2 (°C)	Tc (°C)							
			Tube Profile (mm)							
20			0	10	20	30	38	40	50	60
15	101	170	144	178	199	211	215	214	195	144
15	99	173	161	194	212	222	221	220	198	145
15	100	174	165	197	216	219	216	215	184	146
15	100	174	175	203	218	224	220	218	196	147
15	100	172	159	183	206	218	220	221	203	151
15	100	171	150	182	208	220	221	221	202	153
15	100	170	150	187	210	218	221	219	200	147
15	100	170	161	195	212	219	221	220	199	145
15	101	170	160	194	213	219	220	219	190	144
15	101	170	159	195	216	218	221	220	188	145
15	100	170	164	195	211	218	221	220	191	139
15	100	170	163	197	215	220	222	220	189	136

Experimental results at $T_s=220^\circ\text{C}$ and $T_b=100^\circ\text{C}$

EXPERIMENTAL RAW DATA

Duration (min)	T1 (°C)	T2 (°C)	Tc (°C) Tube Profile (mm)							
16			0	10	20	30	38	40	50	60
15	80	153	163	194	214	222	221	221	198	150
15	80	151	164	193	212	222	220	221	198	151
15	79	149	164	192	212	222	220	218	196	148
15	80	148	164	190	210	220	220	219	196	144
15	80	148	163	192	210	220	220	221	196	147
15	80	148	165	194	213	221	221	220	196	145
15	81	148	162	192	210	219	221	220	196	144
15	80	148	162	192	210	219	221	220	196	144
15	80	148	165	193	212	220	221	218	194	146
15	80	147	165	194	213	222	220	220	195	142
15	80	147	165	195	214	222	220	222	198	147
15	80	147	165	195	214	222	221	220	196	147
15	79	147	164	191	211	220	220	216	192	143

Experimental results at $T_s=220^\circ\text{C}$ and $T_b=80^\circ\text{C}$

EXPERIMENTAL RAW DATA

Duration (min)	T1 (°C)	T2 (°C)	Tc (°C)	Tube Profile (mm)							
14				0	10	20	30	38	40	50	60
15	70	173	163	190	207	219	221	221	221	200	151
15	69	173	168	190	208	220	221	221	221	214	155
15	70	172	172	192	204	217	221	221	220	213	148
15	70	170	168	187	207	216	222	222	218	210	158
15	70	169	166	185	205	218	222	222	221	210	161
15	70	169	163	188	204	219	222	222	220	209	163
15	70	168	169	189	204	220	221	221	222	200	153
15	69	167	166	188	202	215	221	221	221	203	155
15	70	167	165	191	202	214	222	222	222	206	151
15	69	167	167	193	203	214	221	221	222	208	160
15	70	167	171	190	203	214	221	221	220	206	154
15	69	167	174	190	208	214	221	221	220	207	155

Experimental results at $T_s=220^\circ\text{C}$ and $T_b=70^\circ\text{C}$

EXPERIMENTAL RAW DATA

Duration (min)	A (Jacket) (°C)	B (Pump) (°C)	C(Line) (°C)	T1 (°C)	T2 (°C)	Tc (°C)	Tube Profile (mm)							
19.27							0	10	20	30	38	40	50	60
15	103	77	64	99	177	181	210	227	236	240	240	240	220	159
15	97	78	64	100	176	190	214	237	243	240	241	241	223	177
15	93	77	66	100	176	190	213	233	244	241	241	240	222	180
15	87	79	62	99	174	198	222	239	245	241	241	240	203	162
15	83	79	62	99	173	192	218	236	245	240	240	239	207	157
15	85	80	66	101	172	193	220	236	245	241	241	240	211	150
15	88	80	65	101	171	195	226	241	243	241	241	240	210	150
15	91	80	65	101	171	203	229	243	249	241	241	240	204	151
15	84	80	64	99	169	197	225	240	247	241	241	241	203	152
15	85	80	67	100	169	206	229	244	245	241	241	240	204	142
15	88	81	66	100	169	205	230	245	245	240	240	240	203	149
15	89	79	66	100	169	205	230	246	246	241	241	240	211	147

Experimental results at $T_s=240^\circ\text{C}$ and $T_b=100^\circ\text{C}$

EXPERIMENTAL RAW DATA

Duration (min)	T1 (°C)	T2 (°C)	Tc (°C) Tube Profile (mm)							
13			0	10	20	30	38	40	50	60
15	79	166	177	208	231	241	241	241	216	161
15	80	169	178	209	232	241	243	242	218	162
15	79	167	181	213	234	244	243	245	220	166
15	79	166	178	211	234	245	245	247	221	165
15	80	166	177	207	230	244	247	245	222	165
15	80	165	179	210	235	245	247	248	223	168
15	80	167	181	213	238	250	249	250	224	167
15	81	167	181	214	238	250	251	250	225	169
15	80	159	176	208	229	237	240	239	211	156
15	81	155	176	208	230	239	240	239	210	155
15	80	154	176	209	231	240	240	239	211	155
15	80	152	175	209	232	241	239	238	210	154
15	81	153	176	209	232	242	240	238	210	154

Experimental results at Ts=240°C and Tb=80°C

EXPERIMENTAL RAW DATA

Duration (min)	A (Jacket) (°C)	B (Pump) (°C)	C(Line) (°C)	T1 (°C)	T2 (°C)	Tc (°C)	Tube Profile (mm)							
14							0	10	20	30	38	40	50	60
15	88	77	53	70	197	194	214	230	239	241	239	205	161	
15	86	78	39	71	197	194	215	231	239	240	240	214	169	
15	92	78	37	69	197	200	222	236	242	241	240	213	165	
15	91	79	46	70	196	199	224	239	240	240	239	207	166	
15	94	78	45	70	195	200	226	242	243	241	241	213	161	
15	89	80	42	71	195	205	227	244	241	241	241	214	165	
15	83	78	41	71	194	206	233	244	246	241	240	200	153	
15	93	80	39	69	193	207	232	242	245	240	240	203	155	
15	87	81	39	70	192	204	231	242	244	241	240	206	151	
15	90	80	39	69	191	208	231	243	244	239	238	208	160	
15	83	80	40	70	191	207	231	243	244	240	239	204	154	
15	94	78	40	69	191	208	233	248	244	240	239	204	155	

Experimental results at Ts=240°C and Tb=70°C